DOI: 10.1002/ejic.200901205

Formation of Silica Nanolayers on ZnO Electrodes in Dye-Sensitized Solar Cells

Shintaro Ueno[a] and Shinobu Fujihara*[a]

Keywords: Photovoltaic materials / Semiconductors / Nanostructures / Sol–gel processes

Zinc oxide electrodes for use in dye-sensitized solar cells were coated with thin silica layers by using a sol–gel transformation of tetraethylorthosilicate (TEOS). Coating solutions were prepared by mixing TEOS and diluted ammonia while stirring and ultrasonificating simultaneously. Two kinds of coating methods (immersing and dip-coating) were adopted and compared to control the thickness of the silica layers on a nanometer scale. With the immersing method a relatively thick SiO_2 coating was made on zinc oxide particles on the electrodes, which resulted in an increase in the open-circuit photovoltage (V_{oc}) and a large decrease in the short-circuit photocurrent density (J_{sc}). In contrast, by using the dip-coating method, with a relatively low withdrawal speed of 100 $\mu m s^{-1}$, thinner SiO_2 layers could be formed on the zinc oxide particles and a high J_{sc} as well as a high V_{oc} was obtained. These results demonstrate that the V_{oc} characteristics of solar cells using silica-coated zinc oxide electrodes can be enhanced by controlling the structure of the silica-coating layers.

Introduction

Wurtzite-type ZnO is an n-type semiconductor with a direct and wide band gap of 3.37 eV. ZnO shows a high mobility of electrons in the conduction band due to largely overlapping Zn 4s orbitals. These characteristics have made ZnO an attractive material for use in a variety of electronic and optical devices including transparent conductive films,[1] chemical sensors,[2] phosphor screens,[3] and semiconductor layers of dye-sensitized solar cells (DSSCs).[4–6] DSSCs are recognized as promising photovoltaic devices because of their potentially low manufacturing cost and high light-to-electricity conversion efficiency. Although TiO_2 is the material currently used for semiconductor layers of DSSCs, we are focusing on ZnO as the alternative because of their similar band-gap and flat-band potential. Moreover, ZnO has much higher electron mobility than TiO_2.[7–9]

The performance of DSSCs depends largely on the microstructure of the semiconductor electrodes because they work on the basis of photophysical and photochemical processes occurring at interfaces between electrodes and surrounding electrolytes. ZnO exhibits excellent controllability of morphology under low-temperature synthetic procedures, which allows us to elaborate a certain morphology suitable for DSSCs. Recently, we have succeeded in fabricating ZnO-based DSSCs showing a high short-circuit photocurrent density (J_{sc} = 18.11 $mA cm^{-2}$) by employing nanocrystalline pastes containing layered hydroxide zinc acetate (LHZA, also known as layered basic zinc acetate).[6] However, the performance of our ZnO-based DSSC still remains lower than that of the TiO_2-based cells due mainly to a large difference in open-circuit photovoltages (V_{oc}) (approximately 0.6 V for our cell and 0.8 V for TiO_2-based cells).

An ideal V_{oc} value corresponds to the difference between the Fermi level of electrons in the semiconductor and the redox potential of the electrolyte.[10–12] However, many factors exist that decrease the V_{oc} value.[12] It is believed that the lower V_{oc} is due to the capturing of photogenerated electrons by oxidized species (I_3^-) in the electrolyte, which is known as the recombination process. The relationship between V_{oc} and the recombination rate constant k_b is presented by Equation (1),[13]

$$V_{oc} = \left(\frac{kT}{e}\right)\ln\left(\frac{I_{inj}}{n_{cb}k_b[I_3^-]}\right) \quad (1)$$

where k is the Boltzmann constant, T is the temperature, e is the electron charge, I_{inj} is the injection flux, n_{cb} is the density of electrons in the conduction band, and $[I_3^-]$ is the concentration of oxidized species. According to this relationship, one of the strategies to improve V_{oc} is the reduction of k_b, which is expected to be achieved by suppressing the recombination reaction. Therefore, we have tried to construct an energy barrier at the electrolyte/photoanode interface, which may be full of recombination sites, in order to decrease the recombination rate.[14–16] Such an energy barrier can be realized by coating insulators or high flat-band potential semiconductors on the ZnO electrode.[17] In this case, the injection of electrons from dyes to

[a] Department of Applied Chemistry, Keio University,
3-14-1 Hiyoshi, Kohoku-ku, Yokohama 223-8522, Japan
Fax: +81-45-566-1551
E-mail: shinobu@applc.keio.ac.jp

electrodes occurs by the tunneling mechanism. This phenomenon is influenced by the thickness of the coating layers. A larger thickness will decrease J_{sc} because the probability of the electron injection exponentially decreases with the barrier thickness.[18] The structure of the coating layers should therefore be sufficiently thin over the ZnO particles present on the electrode.

In the present study amorphous silica (SiO_2) was employed as the coating layer. We adopted two kinds of coating procedures based on the sol–gel transformation, namely, immersing and dip-coating. Coating solutions were prepared from tetraethylorthosilicate (TEOS) and a diluted ammonia solution.[19] Diluted ammonia works as the catalyst for the following hydrolysis and condensation reactions, see Equations (2) and (3).[20]

$$Si(OC_2H_5)_4 + nOH^- \rightarrow Si(OC_2H_5)_{4-n}(O^-)_n + nC_2H_5OH \quad (2)$$

$$\equiv Si–OH + O^–Si\equiv \rightarrow \equiv Si–O–Si\equiv + OH^- \quad (3)$$

These procedures were applied to our ZnO films, which were prepared by the chemical bath deposition of LHZA and subsequent heat treatments.[4] We then succeeded in making core (ZnO)–shell (silica) structures without destroying the original flower-like ZnO morphology. Another advantage of the silica coating on ZnO may be enhanced durability against aging degradation, which is also discussed in terms of the V_{oc} characteristics.

Results and Discussion

Silica-Coating Conditions

The factors influencing the formation and structure of the silica nanolayers were the first to be examined. Commercial ZnO particles were then coated with silica by using a solution consisting of TEOS, diluted ammonia, and ion-exchanged water. Figure 1 shows the transmission electron microscope (TEM) images of the silica-coated ZnO nanoparticles after changing the coating period or TEOS concentration. The formation of a core–shell structure can be seen in Figure 1. In the samples shown in Figure 1 (a–c), the coating period was varied among 1.5, 3, and 6 h while a volume ratio of TEOS to ion-exchanged water was fixed at 0.1. Because the initial ZnO particles were approximately 20 nm in size, the dark-contrast particles surrounded by light-contrast layers correspond to ZnO (core)–silica (shell) structures. The samples shown in Figure 1 (d–f) were obtained by changing the volume ratio of TEOS to ion-exchanged water among 0.004, 0.01, and 0.02 at a fixed coating period of 1.5 h. Thin layers up to 5 nm in thickness are clearly observed in these magnified TEM images.

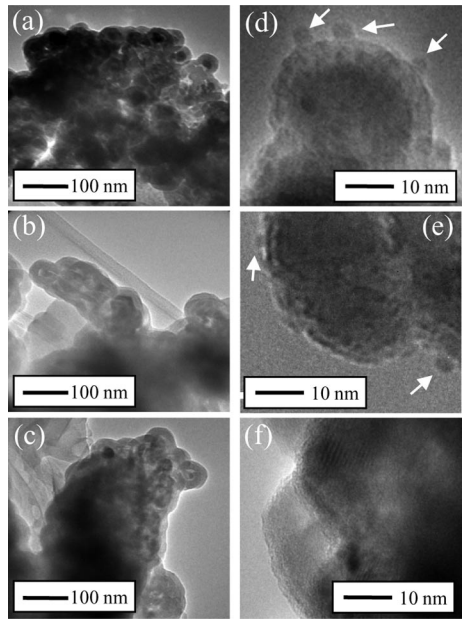

Figure 1. TEM images of the silica-coated ZnO particles. On the left side, the amount of TEOS was fixed at 2500 μL and the coating period was varied among (a) 1.5 h, (b) 3 h, and (c) 6 h. On the right side, the coating period was fixed at 1.5 h and the TEOS/water volume ratio was varied among (d) 0.02, (e) 0.01, and (f) 0.004.

The core–shell structure is assumed to be made from the reaction between surface OH groups of the ZnO particles and the hydrolyzed TEOS. This reaction might proceed very rapidly due to lower stability of TEOS in the aqueous medium, leading to heterogeneous nucleation occurring preferentially on the ZnO surface at the initial reaction stage. Small dots (ca. 5 nm) observed on the coating layer in Figure 1 (see d, e), as indicated by arrows, are considered to be spherical silica particles since we confirmed their formation from this solution even in the absence of the ZnO particles. Accordingly, because of the long coating periods and the relatively high TEOS concentration, the silica particles were formed through homogeneous precipitation in the solution and attached to the silica-coating layers. As a result of these experiments we could obtain a relationship between the nanolayer thickness and the coating period or the TEOS concentration as shown in Figure 2. The thickness increases

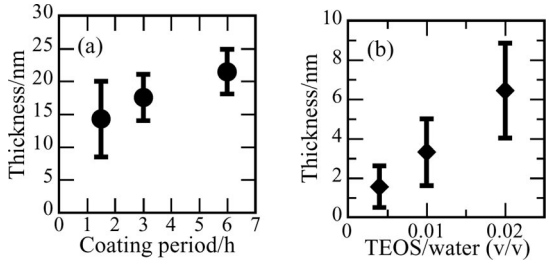

Figure 2. The relationship between the thickness of the silica layer and (a) the coating period (the TEOS/water ratio was 0.1) or (b) the TEOS/water volume ratio (the coating period was 1.5 h).

simply by increasing the coating period or the TEOS concentration. We can then precisely control the thickness of the SiO_2 coating on the ZnO electrodes as described below.

Silica Coating by the Immersing Method

The relationship in Figure 2 indicates that the appropriate coating period should be less than 1.5 h in order to obtain thinner SiO_2 layers that are a few nanometers in thickness. This is because a larger thickness would decrease the probability of the electron injection and hence J_{sc}.[18] In this regard the volume ratio of TEOS to ion-exchanged water should be between 0.001 and 0.004. The composition was therefore varied over this range to examine the formation of silica nanolayers on the ZnO electrodes. Table 1 summarizes the solution composition used here. Solutions are denoted as S-0, S-20, S-40, and S-80. Electrodes coated by the immersing method using these solutions are designated as I-0, I-20, I-40, and I-80, respectively. The S-0 solution and the I-0 electrode were used as a reference without the silica coating. The coating period was fixed at 0.5 h. The dye-loading condition for these electrodes, for use in DSSCs, was also optimized with immersing at 60 °C for 2 h. The thickness of the ZnO films was 30–35 μm.

Table 1. The composition of the TEOS coating solutions.

Solution	Water [mL]	TEOS [μL]	NH_3(aq) [μL]
S-0	20	0	500
S-20	20	20	500
S-40	20	40	500
S-80	20	80	500

The presence of silica nanolayers on the electrodes was first confirmed by an X-ray photoelectron spectroscopy (XPS) analysis. Figure 3 shows XPS spectra in the Si 2p region. A peak from the Si 2p electrons is clearly observed at a binding energy of approximately 102 eV for the I-40 and I-80 electrodes, indicating the presence of silica. On the other hand, no peak is observed for the I-20 sample. The silica nanolayers of the I-40 and I-80 electrodes could also be observed by the TEM analysis, as shown in Figure 4. The silica layer covers each ZnO particle well, like a core–shell structure. The thickness of the silica nanolayer is 1–3 nm on the I-40 and 4–6 nm on the I-80 electrode. This difference reflects the TEOS concentration of the coating solutions. As for the I-20 electrode, we could not detect silica layers, at least not from the XPS and TEM analyses.

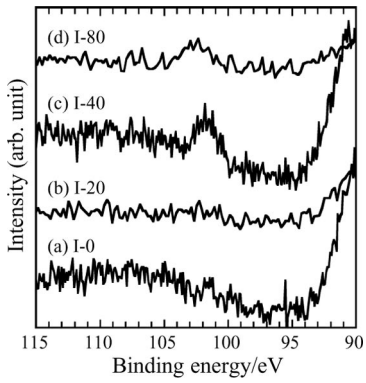

Figure 3. XPS spectra in the Si 2p region for (a) the uncoated film of I-0 and the coated films of (b) I-20, (c) I-40, and (d) I-80.

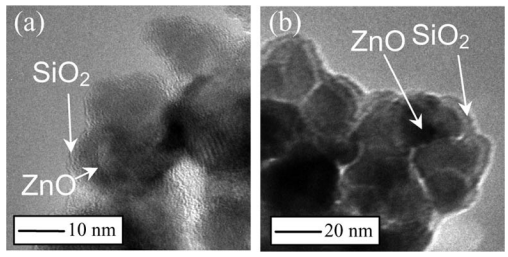

Figure 4. TEM images of (a) the I-40 and (b) the I-80 film.

Photocurrent density–voltage curves (*J*–*V* curves) and dark current–voltage curves of the silica-coated electrodes are shown in Figure 5. The characteristics of the cells [V_{oc}, J_{sc}, fill factor (*ff*), and the conversion efficiency (η)] are summarized in Table 2. Notably the V_{oc} value increases from 0.676 V for the I-0 to 0.751 V for the I-40 electrode, in accordance with the increase in the TEOS concentration in the solution. In contrast, the I-80 electrode shows a decreased V_{oc} value of 0.690 V. This electrode also has relatively low J_{sc}, *ff*, and hence η values. The silica layer was therefore too thick to inject photo-excited electrons from dyes onto ZnO for the I-80 electrode. In addition, the silica layer might disturb the adsorption of dyes because the surface of SiO_2 tends to be negatively charged because of the relatively low point of zero charge.[21] The surface silanol

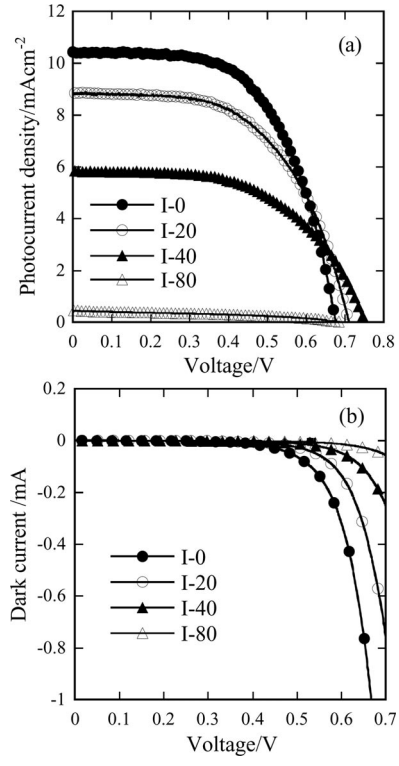

Figure 5. (a) *J*–*V* curves and (b) dark current–voltage curves of the cells using the ZnO electrodes coated with SiO_2 by the immersing method.

groups can then repel the deprotonated dyes with anchoring carboxyl groups. This can explain the decrease in the amount of adsorbed dyes in Table 2. Judging from the decrease in J_{sc}, the I_{inj} value may also decrease due to the presence of the insulating silica layer, which would have a negative effect on V_{oc} according to Equation (1). Nonetheless the V_{oc} is increased by the SiO_2 coating, indicating that the recombination rate could be reduced. This is supported by the data in Figure 5 (b), which shows the dark current–voltage curves of the electrodes. With the applied voltage above 0.4 V, the dark currents of the SiO_2-coated electrodes are much lower than that of the uncoated electrode. This fact implies that the kinetics[16] of the charge transfer to the electrolyte (recombination) is much slower for the I-20 to I-80 electrodes. For the further enhancement of the overall conversion efficiency, the recovery of the decreased J_{sc} is indispensable.

Table 2. The characteristics of the cells using the ZnO electrodes coated with SiO_2 by the immersing method.

Electrode	V_{oc} [V]	J_{sc} [mA cm^{-2}]	*ff*	η [%]	Adsorbed dye [$\times 10^{-7}$ mol cm^{-2}]
I-0	0.676	10.43	0.596	4.20	1.81
I-20	0.711	8.84	0.563	3.54	1.80
I-40	0.751	5.82	0.557	2.44	1.70
I-80	0.690	0.442	0.393	0.12	1.63

Silica Coating by the Dip-Coating Method

The dip-coating is a powerful method that is available for immediately coating objects, even if they are on a nanometer scale and have large specific surface areas. The thickness of the silica nanolayers is expected to be more easily defined in the dip-coating process, because there are many controllable factors to dominate the coating-layer structure such as the withdrawal speed, the solution concentration, the viscosity, and so forth. We carried out the dip-coating by using the coating solution described above (S-0, S-20, S-40, and S-80) with a relatively low withdrawal speed of 100 μm s^{-1} to obtain thin silica layers. The coated electrodes were then immersed in the 0.3 mM N719 solution at 60 °C for 30 min. The resultant photoanodes are designated as D-0, D-20, D-40, and D-80 after the coating solutions of S-0, S-20, S-40, and S-80, respectively. The thickness of all the coated ZnO films was 35 μm.

In contrast to the immersing method, the presence of silica layers could not be clearly confirmed by the XPS analysis. That is, only the D-80 electrode showed a very weak peak at 101.6 eV. Also in the TEM study, we could not distinguish a surface silica nanolayer from the ZnO particle in the images. These experimental facts imply that the silica layers are present but are very thin, or not formed on the ZnO particle. We then tried to detect silica on the electrode by a Fourier transform infrared spectroscopy (FTIR) analysis. Figure 6 compares FTIR spectra of the electrodes coated by the immersion and the dip-coating method. At a high wavenumber range, between 3500 and 3100 cm^{-1}, a broad absorption band is observed resulting from the stretching vibration modes of the hydroxy group (O–H) for all the samples. A band at 1640 cm^{-1} may come from water from the solutions. Absorption peaks from the C–H vibrations also appear at 2950–2850 and 1400 cm^{-1}. Peaks at a lower wavenumber, ranging between 880 and 830 cm^{-1}, are attributed to bending vibrations of Si–OH. Therefore, the samples contain TEOS-derived residues. It is known that the absorption by the Si–O–Si transverse optical (TO) mode appears at 1020 cm^{-1}.[22] Because an absorption peak is clearly observed at this wavelength for the I-20, I-40, I-80, D-40, and D-80 electrodes, we tentatively conclude that the silica nanolayers are also formed on the dip-coated electrodes. But the amount of silica on the dip-coated electrodes is smaller than that on the electrodes coated by the immersion. These qualitative and quantitative results are consistent with the TEOS concentration and the TEM observation.

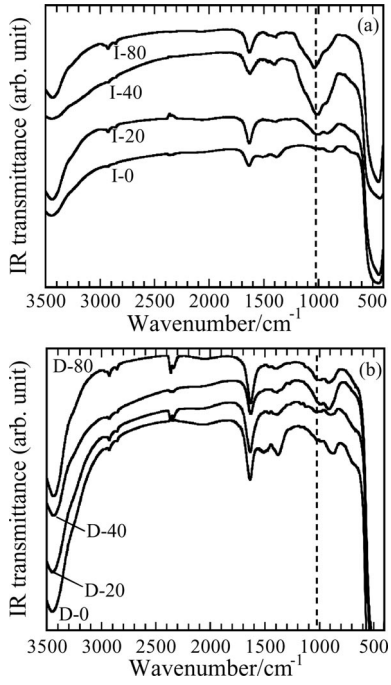

Figure 6. FTIR spectra of (a) the I-0 to I-80 films and (b) the D-0 to D-80 films. The dashed line shows the location of the Si–O–Si TO mode peak.

J–*V* curves and dark current–voltage curves of the D-0, D-20, D-40, and D-80 electrodes are shown in Figure 7. The characteristics of the cells are summarized in Table 3. Obviously the *J*–*V* characteristics of the dip-coated electrodes are very different from those of the electrodes coated by immersion. Especially, the J_{sc} values are much higher in the dip-coated electrodes. It is considered that the dip-coating gives thinner silica layers and hence the tunneling of photo-excited electrons from dyes to ZnO is less disturbed, leading to the higher J_{sc} values. An increase in V_{oc} is observed for the D-40 and D-80 electrodes, while the V_{oc} for the D-0 and D-20 electrodes remains low. The relatively small dark current of the D-40 and D-80 electrodes shown in Figure 7 (b) agrees with the V_{oc} behavior. The reason for the first decrease of V_{oc} from D-0 to D-20 and its increase from D-20 to D-40 can be explained as follows. As seen

from Figure 7 (b), the dark current of the D-20 electrode is larger than that of the D-0 electrode, which indicates that the back-electron transfer is more frequent in D-20. The formation of the silica nanolayer is insufficient in D-20, while the amount of the adsorbed dye is decreased from D-0. Because the presence of dye can also suppress the back-electron transfer, the D-20 electrode has the lowest V_{oc} value among the present samples. The above experimental facts demonstrate that the sufficiently coated silica nanolayers act as the energy barrier to suppress the recombination and increase the V_{oc}. Moreover, the degree of the decrease in J_{sc} with increasing the TEOS concentration in the dip-coated electrodes is smaller than that in the electrodes coated by immersion.

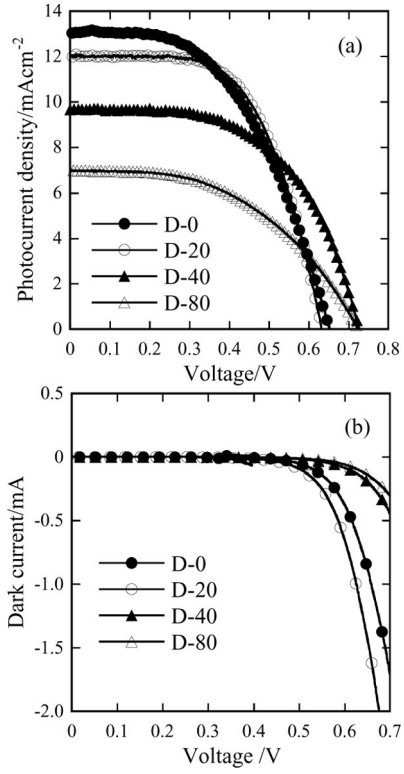

Figure 7. (a) J–V curves and (b) dark current–voltage curves of the cells using the ZnO electrodes coated with SiO_2 by the dip-coating method.

Table 3. The characteristics of the cells using the ZnO electrodes coated with SiO_2 by the dip-coating method.

Electrode	V_{oc} [V]	J_{sc} [mA cm^{-2}]	ff	η [%]	Adsorbed dye [$\times 10^{-7}$ mol cm^{-2}]
D-0	0.653	13.03	0.507	4.31	1.17
D-20	0.632	12.00	0.598	4.54	1.03
D-40	0.726	9.67	0.562	3.95	0.97
D-80	0.724	6.96	0.487	2.46	1.04

Finally, it is noteworthy that the unique, flower-like morphologies of the as-prepared ZnO films are maintained after the silica coating treatment, as shown in scanning electron microscopy (SEM) images of the I-40 and the D-40 electrode (Figure 8). Because the TEOS coating solution is basic, the formation of the silica nanolayers is effective in preventing the dissolution of the ZnO particles. This is expected to be helpful in enhancing the durability of the ZnO photoanodes during the cell operation. Figure 9 shows results of the durability test for the cells using the uncoated and the coated I-40 electrode. The rate of change in V_{oc} and J_{sc} was plotted against time when the J–V measurement was carried out. It is clearly seen that the V_{oc} values of the I-40 electrode are higher than those of the uncoated electrode, as expected. The first increase in V_{oc} from 0 to 24 h is attributed to the stabilization of the cell because of sufficient penetration of the electrolyte onto the electrode, which is usually observed in DSSCs. On the contrary, the J_{sc} values decrease faster for the I-40 electrode. As mentioned above, the silica layer may disturb the dye adsorption, which leads to a detachment of dyes during the cell operation. In this regard other metal oxides should be explored that will not deteriorate the photocurrent.

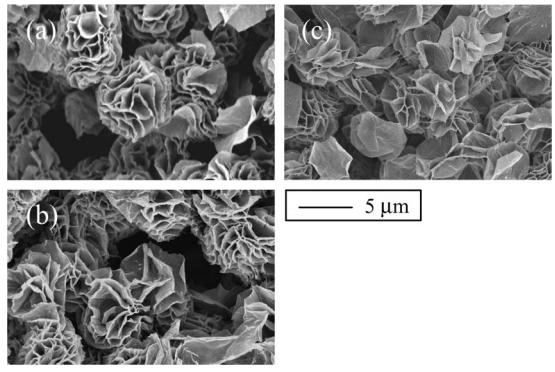

Figure 8. SEM images of (a) the uncoated ZnO, (b) the I-40, and (c) the D-40 film.

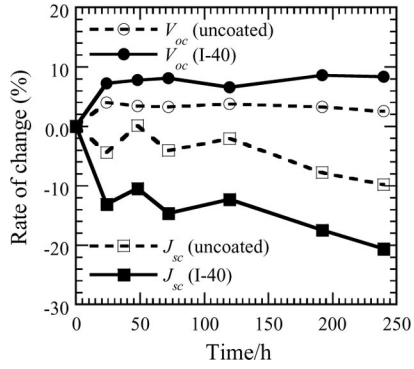

Figure 9. The rate of change in V_{oc} and J_{sc} of the cells using the uncoated and the coated (I-40) ZnO electrode, plotted against time for the J–V measurement in the durability test.

Conclusions

The silica nanolayers were formed on the ZnO electrodes as the energy barrier by the simple sol–gel transformation using the immersing or the dip-coating method. The thickness of the silica nanolayers could be controlled by the coating period and the TEOS concentration in the solutions.

The presence of the silica nanolayers greatly influenced the *J*–*V* characteristics of the ZnO-based DSSCs. In particular, we could control the V_{oc} values by changing the solution composition and the coating method. The maximum V_{oc} of 0.751 V was achieved by the immersing method, whereas the J_{sc} and the conversion efficiency η decreased due to the disturbed injection of photo-excited electrons by the thicker silica nanolayers. We then tried the dip-coating method using the same solutions and achieved a V_{oc} value of 0.726 V without decreasing the J_{sc} value, leading to a conversion efficiency of η = 3.95%. Our results demonstrate that ZnO is still promising as an alternative to TiO_2 by appropriate modification of the electrode structure. Work is ongoing to look for better coating conditions to further improve the performance of ZnO-based DSSCs.

Experimental Section

Silica Nanolayers: We first examined factors influencing the formation and structure of silica nanolayers. Commercial ZnO nanoparticles (5.0 g; Sakai Chemical Industry Co., Ltd., Japan) were dispersed in a coating solution consisting of TEOS (2500 μL; Wako Pure Chemicals Co., Ltd., Japan), diluted ammonia (0.625 mL; Wako), and ion-exchanged water (25 mL). The resultant solution was stirred for 1.5, 3, or 6 h. These periods are denoted as "coating periods". Next, the coating period was fixed at 1.5 h while a volume ratio of TEOS to ion-exchanged water was changed among 0.004, 0.01, and 0.02 (amounts of diluted ammonia and ion-exchanged water were kept the same). Silica-coated ZnO nanoparticles were collected by centrifugation and washed with ethanol and ion-exchanged water. The washing process was repeated twice.

ZnO Films: Experimental procedures for preparing ZnO films followed our previous reports based on the chemical-bath deposition and subsequent heating processes.[23,24] Zinc acetate dihydrate [0.15 M; $Zn(CH_3COO)_2{\cdot}2H_2O$; 99.9% purity, Wako] was dissolved in anhydrous methanol. Fluorine-doped tin oxide-coated glass substrates (FTO glass substrates) (Nippon Sheet Glass Co., Ltd.; sheet resistance of 10 Ω/square) were immersed in the resultant solution and kept at 60 °C for 30 h in a dry-block bath. Films of layered hydroxide zinc acetate (LHZA) were deposited on both sides of the substrates. The unnecessary film on the bottom side was removed by scratching. The films were heat-treated at 450 °C for 10 min and then quenched to room temperature. Thus ZnO films having a flower-like morphology were formed on the FTO substrates.

SiO_2 Coating: TEOS and diluted ammonia were mixed by an ultrasonic stirrer (USS-1, Nihonseiki Kaisha Ltd., Japan), which could stir the solution under ultrasonification treatment. Two kinds of coating procedures were tested and compared. On the one hand, the ZnO films obtained above were immersed in the solution for a certain period (the immersing treatment). On the other hand, the solution was dip-coated on the ZnO films using a micro-speed dip coater (MS215, Asumi Giken Ltd., Japan) (the dip-coating treatment). The TEOS concentration was changed to examine the influence of solution compositions on the structure of silica nanolayers and hence the solar cell performance. After the coating procedures, the silica-coated ZnO films were carefully rinsed with ethanol and ion-exchanged water and dried at room temperature.

Dye-loading onto the silica-coated ZnO films was carried out by immersing them in a 0.3 mM N-719 [$RuL_2(NCS)_2$:2TBA; L = 2,2′-bipyridyl-4,4′-dicarboxylic acid and TBA = tetrabutylammonium] ethanolic solution at 60 °C to obtain photoanodes of DSSCs.

Characterization: The structure of silica nanolayers was examined by TEM (FEI Tecnai Spirits), XPS (JEOL JPS-900MC and JPS 9000MX), and FTIR spectroscopy (Bruker ALPHA). The films were scratched and the resultant powders were mixed with KBr to record the FTIR spectra. The morphology of the electrodes was observed by SEM (FEI Sirion).

Sandwich-type open cells were constructed with the ZnO/N-719 photoanode, the I^-/I_3^- redox-couple electrolyte, the spacer film, and the counter-platinum electrode. The electrolyte was composed of 0.1 M LiI, 50 mM I_2, 0.6 M 1,2-dimethyl-1,3-propyl-imidazolium iodide, 1 M *tert*-butylpyridine, and 3-methoxypropionitrile. The performance (V_{oc}, J_{sc}, *ff*, and η) of the DSSCs thus obtained was evaluated by *J*–*V* measurements. The active cell area was 0.25 cm^2, regulated by a mask. A 500 W Xe lamp (Ushio UXL-500SX) was used as the light source to produce the AM 1.5 illumination at 100 mW cm^{-2} (1 sun). An AM 1.5 filter, a water filter, and an infrared cut filter (Hoya S76-HA50) were placed in the light path to regulate light over the wavelength range of 300–800 nm and reduce the mismatch between the simulated sunlight and AM 1.5. Dark current–voltage curves were also measured in the same way under the dark conditions.

The amount of dyes adsorbed on the electrode was determined by removing them in a 0.5 M NaOH ethanol/water solution. The absorbance of the resultant dye solution was measured by a UV/Vis spectrophotometer (Hitachi U-3300) and calibrated with standard solutions of N-719.

Acknowledgments

This work was supported by Keio Gijuku Academic Development Funds.

[1] T. Minami, H. Nanto, S. Takata, *Jpn. J. Appl. Phys.* **1984**, *23*, L280–L282.
[2] K. S. Weißenrieder, J. Müller, *Thin Solid Films* **1997**, *300*, 30–41.
[3] L. E. Greene, M. Law, J. Goldberger, F. Kim, J. C. Johnson, Y. Zhang, R. J. Saykally, P. Yang, *Angew. Chem. Int. Ed.* **2003**, *42*, 3031–3034.
[4] K. Kakiuchi, E. Hosono, S. Fujihara, *J. Photochem. Photobiol. A: Chem.* **2006**, *179*, 81–86.
[5] H. Rensmo, K. Keis, H. Lindström, S. Södergren, A. Solbrand, A. Hagfeldt, S. E. Lindquist, L. N. Wang, M. Muhammed, *J. Phys. Chem. B* **1997**, *101*, 2598–2601.
[6] M. Saito, S. Fujihara, *Energy Environ. Sci.* **2008**, *1*, 280–283.
[7] M. Grätzel, *Nature* **2001**, *414*, 338–344.
[8] M. Quintana, T. Edvinsson, A. Hagfeldt, G. Boschloo, *J. Phys. Chem. C* **2007**, *111*, 1035–1041.
[9] H. G. Agrell, G. Boschloo, A. Hagfeldt, *J. Phys. Chem. B* **2004**, *108*, 12388–12396.
[10] B. O'Regan, M. Grätzel, *Nature* **1991**, *353*, 737–740.
[11] M. Grätzel, *Inorg. Chem.* **2005**, *44*, 6841–6851.
[12] S. Y. Huang, G. Schlichthörl, A. J. Nozik, M. Grätzel, A. J. Frank, *J. Phys. Chem. B* **1997**, *101*, 2576–2582.
[13] M. K. Nazeeruddin, A. Kay, I. Rodicio, R. Humphry-Baker, E. Müller, P. Liska, N. Vlachopoulos, M. Grätzel, *J. Am. Chem. Soc.* **1993**, *115*, 6382–6390.
[14] Y. Diamant, S. G. Chen, O. Melamed, A. Zaban, *J. Phys. Chem. B* **2003**, *107*, 1977–1981.
[15] Y. Diamant, S. Chappel, S. G. Chen, O. Melamed, A. Zaban, *Coord. Chem. Rev.* **2004**, *248*, 1271–1276.
[16] S. G. Chen, S. Chappel, Y. Diamant, A. Zaban, *Chem. Mater.* **2001**, *13*, 4629–4634.

[17] M. Law, L. E. Greene, A. Radenovie, T. Kuykendall, J. Liphardt, P. Yang, *J. Phys. Chem. B* **2006**, *110*, 22652–22663.
[18] P. K. M. Bandaranayake, P. V. V. Jayaweera, K. Tennakone, *Sol. Energy Mater. Sol. Cells* **2003**, *76*, 57–64.
[19] P. Yang, M. Ando, N. Murase, *J. Colloid Interface Sci.* **2007**, *316*, 420–427.
[20] C. J. Brinker, *J. Non-Cryst. Solids* **1988**, *100*, 31–50.
[21] E. Palomares, J. N. Clifford, S. A. Haque, T. Lutz, J. R. Durrant, *J. Am. Chem. Soc.* **2003**, *125*, 475–482.
[22] S. Mukherjee, A. K. Pal, *J. Phys. Condens. Matter* **2008**, *20*, 255202.
[23] E. Hosono, S. Fujihara, T. Kimura, *J. Mater. Chem.* **2004**, *14*, 881–886.
[24] E. Hosono, S. Fujihara, T. Kimura, *Electrochim. Acta* **2004**, *49*, 2287–2293.

Received: December 14, 2009
Published Online: April 8, 2010

